





## Article

# Selenium Yeast and Fish Oil Combination Diminishes Cancer Stem Cell Traits and Reverses Cisplatin Resistance in A549 Sphere Cells

I-Chun Lai <sup>1,2,3</sup>, Chien-Huang Liao <sup>4</sup>, Ming-Hung Hu <sup>4,5</sup> , Chia-Lun Chang <sup>4,5,6</sup>, Gi-Ming Lai <sup>4,5</sup>, Tzeon-Jye Chiou <sup>4,5</sup> , Simon Hsia <sup>7</sup>, Wei-Lun Tsai <sup>4</sup>, Yu-Yin Lin <sup>4</sup>, Shuang-En Chuang <sup>8</sup>, Jacqueline Whang-Peng <sup>4,5</sup>, Hsuan-Yu Chen <sup>1,9,10,11,12,13,\*</sup>  and Chih-Jung Yao <sup>6,14,\*</sup> 

- <sup>1</sup> The Ph.D. Program for Translational Medicine, College of Medical Science and Technology, Taipei Medical University and Academia Sinica, Taipei 11031, Taiwan
  - <sup>2</sup> Division of Radiation Oncology, Department of Oncology, Taipei Veterans General Hospital, Taipei 11217, Taiwan
  - <sup>3</sup> School of Medicine, National Yang Ming Chiao Tung University, Taipei 11230, Taiwan
  - <sup>4</sup> Cancer Center, Wan Fang Hospital, Taipei Medical University, Taipei 11696, Taiwan
  - <sup>5</sup> Division of Hematology and Medical Oncology, Department of Internal Medicine, Wan Fang Hospital, Taipei Medical University, Taipei 11696, Taiwan
  - <sup>6</sup> Department of Internal Medicine, School of Medicine, College of Medicine, Taipei Medical University, Taipei 11031, Taiwan
  - <sup>7</sup> Taiwan Nutraceutical Association, Taipei 10596, Taiwan
  - <sup>8</sup> National Institute of Cancer Research, National Health Research Institutes, Miaoli 35053, Taiwan
  - <sup>9</sup> Ph.D. Program for Translational Medicine, National Taiwan University, Taipei 10051, Taiwan
  - <sup>10</sup> Genome and Systems Biology Degree Program, National Taiwan University, Taipei 10051, Taiwan
  - <sup>11</sup> Ph.D. Program in Microbial Genomics, National Chung Hsing University, Taichung 40227, Taiwan
  - <sup>12</sup> Department of Medical Research, Kaohsiung Medical University Hospital, Kaohsiung 80761, Taiwan
  - <sup>13</sup> Institute of Statistical Science, Academia Sinica, Taipei 11529, Taiwan
  - <sup>14</sup> Department of Medical Education and Research, Wan Fang Hospital, Taipei Medical University, Taipei 11696, Taiwan
- \* Correspondence: hychen@stat.sinica.edu.tw (H.-Y.C.); yaochihjung@gmail.com (C.-J.Y.)



**Citation:** Lai, I.-C.; Liao, C.-H.; Hu, M.-H.; Chang, C.-L.; Lai, G.-M.; Chiou, T.-J.; Hsia, S.; Tsai, W.-L.; Lin, Y.-Y.; Chuang, S.-E.; et al. Selenium Yeast and Fish Oil Combination Diminishes Cancer Stem Cell Traits and Reverses Cisplatin Resistance in A549 Sphere Cells. *Nutrients* **2022**, *14*, 3232. <https://doi.org/10.3390/nu14153232>

Academic Editors: Dariusz Nowak, Anthony Perkins and James Cuffe

Received: 6 June 2022

Accepted: 28 July 2022

Published: 7 August 2022

**Publisher's Note:** MDPI stays neutral with regard to jurisdictional claims in published maps and institutional affiliations.



**Copyright:** © 2022 by the authors. Licensee MDPI, Basel, Switzerland. This article is an open access article distributed under the terms and conditions of the Creative Commons Attribution (CC BY) license (<https://creativecommons.org/licenses/by/4.0/>).

**Abstract:** Cisplatin is a prevalent chemotherapeutic agent used for non-small cell lung cancer (NSCLC) that is difficult to treat by targeted therapy, but the emergence of resistance severely limits its efficacy. Thus, an effective strategy to combat cisplatin resistance is required. This study demonstrated that, at clinically achievable concentrations, the combination of selenium yeast (Se-Y) and fish oil (FO) could synergistically induce the apoptosis of cancer stem cell (CSC)-like A549 NSCLC sphere cells, accompanied by a reversal of their resistance to cisplatin. Compared to parental A549 cells, sphere cells have higher cisplatin resistance and possess elevated CSC markers (CD133 and ABCG2), epithelial–mesenchymal transition markers (anexolekto (AXL), vimentin, and N-cadherin), and cytoprotective endoplasmic reticulum (ER) stress marker (glucose-regulated protein 78) and increased oncogenic drivers, such as yes-associated protein, transcriptional coactivator with PDZ-binding motif,  $\beta$ -catenin, and cyclooxygenase-2. In contrast, the proapoptotic ER stress marker CCAAT/enhancer-binding protein homologous protein and AMP-activated protein kinase (AMPK) activity were reduced in sphere cells. The Se-Y and FO combination synergistically counteracted the above molecular features of A549 sphere cells and diminished their elevated CSC-like side population. AMPK inhibition by compound C restored the side population proportion diminished by this nutrient combination. The results suggest that the Se-Y and FO combination can potentially improve the outcome of cisplatin-treated NSCLC with phenotypes such as A549 cells.

**Keywords:** selenium; lung cancer; cisplatin; fish oil; cancer stem cell; AMPK; side population

## 1. Introduction

Lung cancer is the leading cause of cancer-related mortality worldwide, accounting for approximately eighteen percent (1.8 million) of all cancer deaths [1]. Approximately 85% of lung cancers are non-small cell lung cancers (NSCLCs), including adenocarcinoma, squamous cell carcinoma, and large cell carcinoma [2]. The most dominant subtype is lung adenocarcinoma [3]. Despite recent advances in the effectiveness of tyrosine kinase inhibitors and vast chemotherapeutics, drug resistance often occurs after the initial effective treatment, resulting in relapse and fatal outcomes. Evidence indicates the critical contribution of cancer stem cells (CSCs) to drug resistance and eventual treatment failure. Therefore, effective therapeutics to eliminate CSC is urgently required. However, most conventional anticancer drugs fail to effectively eradicate CSCs [4], and some of them have been reported to foster CSC traits [2,5–7]. On the contrary, diverse natural products, including diet-derived nutrients, are known to suppress CSC traits and related signaling molecules, representing a cornucopia of CSC inhibitors [4,8,9]. Nonetheless, most natural products have modest potency and may not be used as a single agent for satisfactory anticancer effects [9]. Therefore, the combination of natural products for more potent anticancer efficacy has been suggested [10–13].

Selenium yeast (Se-Y) and fish oil (FO) are well known as nutrients, and their individual anticancer activities have been widely examined. However, their clinical efficacies are still superficially plausible, and certain clinical trial outcomes are not substantially satisfactory or are even conflicting [14,15]. Remarkably, a previous study reported the synergistic combined effects of Se-Y and FO on apoptosis induction in A549 lung adenocarcinoma cells via AMP-activated protein kinase (AMPK) activation and the opposite regulation of proapoptotic CCAAT/enhancer-binding protein homologous protein (CHOP) and cytoprotective glucose-regulated protein 78 (GRP78) endoplasmic reticulum (ER) stress-response elements, accompanied by a decrease in  $\beta$ -catenin and cyclooxygenase-2 (COX-2) [16]. These targeted molecules (CHOP [17], GRP78 [17,18],  $\beta$ -catenin [19], and COX-2 [20]) are closely associated with gefitinib resistance in lung cancer. Hence, subsequent study employed the Se-Y and FO combination to reverse acquired gefitinib resistance of lung adenocarcinoma HCC827 cells (E746-A750 exon 19 deletion) with elevated GRP78,  $\beta$ -catenin, COX-2, and CSC markers (ABCG2 and CD133), and epithelial–mesenchymal transition (EMT) markers (vimentin and anelexleto (AXL)) [21]. Besides the association with acquired gefitinib resistance [21], the aforementioned CSC and EMT markers have been reported to be involved in the resistance to the widely prescribed chemotherapy agent cisplatin [5,6,22–26]. The suppressing effects of the Se-Y and FO combination on elevated CSC and EMT markers in gefitinib-resistant HCC827 cells [21] imply the capability of reversing cisplatin resistance in lung CSCs. Additionally, AMPK suppression elevates the ATP-dependent efflux pump ABCG2 in A549 cells, increasing the side population of chemoresistant cells [7]. Activation of AMPK by the Se-Y and FO combination in A549 cells [16] is proposed to eliminate the above-described CSC-like side population.

To investigate the valuable potentiality of this nutrient combination, CSC-like A549 sphere cells were enriched and collected by culturing A549 lung adenocarcinoma cells [epidermal growth factor receptor (EGFR) wild-type, KRAS-G12S] as spheroid bodies in a defined small-molecule-based serum-free medium. Consistent with the reported characteristics of sphere cells [27–29], these A549 sphere cells displayed higher CSC and EMT markers and elevated cisplatin resistance. This study explored the combined effects of Se-Y and FO on A549 sphere cells, including CSC trait diminishment, cisplatin resistance reversion, apoptosis induction, ER stress modification, and AMPK activation. Moreover, AMPK inhibits yes-associated protein (YAP) and its paralog, transcriptional coactivator with PDZ-binding motif (TAZ), which are oncogenic drivers conferring CSC traits [30]. The combined effects of Se-Y and FO on YAP and TAZ in CSC-like A549 sphere cells were also studied.

## 2. Materials and Methods

### 2.1. Cell Culture

The A549 human NSCLC cell line was obtained from Bioresource Collection and Research Center (Hsinchu, Taiwan) and cultured in RPMI-1640 medium (Gibco, CA, USA) supplemented with 10% fetal bovine serum (35-010-CV, Corning Incorporated, Corning, NY, USA), 1× penicillin–streptomycin–glutamine (Corning Incorporated, Corning, NY, USA), and 1× nonessential amino acids (Corning Incorporated, Corning, NY, USA). To obtain sphere cultures, A549 cells were seeded at a density of  $2.24 \times 10^7$  cells/10 cm culture dish (150466, Thermo Fisher Scientific, Nunc, Waltham, MA, USA) containing 8 mL PluriSTEM™ human ES/iPS Cell medium (SCM130, Millipore, Burlington, MA, USA) supplemented with 1× penicillin–streptomycin–glutamine. After 24 h, the attached cells were discarded and the floating cells with round and smooth contour were collected, transferred to an uncoated 10 cm dish (70165-102, Corning, Oneonta, NY, USA) at density of  $2 \times 10^6$  cells/dish and cultured with 8 mL PluriSTEM™ human ES/iPS cell medium for another 24 h. In the following 5 days, the growing cells were split 1:1 to expand the number. To keep the conditioned medium, only half of the medium was refreshed upon splitting. The clumping of cells was resolved by trituration without using trypsin/ethylenediaminetetraacetic acid (EDTA). After being cultured for 7 days, the sphere cells were analyzed for their CSC traits and then used for subsequent experiments. Except as specifically depicted in the legends of Figures in Results section, the experiments of A549 sphere cells were performed in uncoated 10 cm dishes with 8 mL PluriSTEM™ human ES/iPS cell medium. The RPMI-1640 medium was supplemented with 10% fetal bovine serum, 1× penicillin–streptomycin–glutamine and 1× nonessential amino acids, and the PluriSTEM™ human ES/iPS cell medium was supplemented with 1× penicillin–streptomycin–glutamine. All cells were maintained in a water-jacketed 5% carbon dioxide (CO<sub>2</sub>) incubator at 37 °C.

### 2.2. Reagents and Chemicals

Se-Y was employed as the form of selenium for the treatment of NSCLC cells. The stated concentration of Se-Y indicates the content of selenium from selenium yeast. The stock solutions of Se-Y and fish oil (FO, each gram contained 220 mg of docosahexaenoic acid (DHA) and 330 mg of eicosapentaenoic acid (EPA)) were obtained from Dr. Chih-Hung Guo (Institute of Biomedical Nutrition, Hung-Kuang University, Taichung, Taiwan). In brief, Se-Y is a mixture of small-molecule peptide-bound selenium extracted from yeast grown in selenium-enriched medium. FO is produced from anchovy by supercritical CO<sub>2</sub> extraction. FO is a mixture of natural triglyceride (TG) form of omega-3 fatty acids. They were then aliquoted, stored at −80 °C (Se-Y) and −20 °C (FO), and diluted in sterile culture medium immediately prior to use. The concentrations of FO depicted in text and figures represent the content of omega-3 fatty acids (DHA and EPA). When combined with cisplatin, Se-Y and FO were added to A549 sphere cells and then the cisplatin was added. Cisplatin was obtained from clinical preparations of Adbluplatin solution (Pharmachemie BV, Haarlem, the Netherlands). DyeCycle Violet (DCV) dye was purchased from Invitrogen (Invitrogen, Carlsbad, CA, USA). Sulforhodamine B (SRB), compound C (also called dorsomorphin, an AMPK inhibitor), propidium iodide, and trichloroacetic acid were bought from Sigma-Aldrich (St. Louis, MO, USA). FITC Annexin V Apoptosis Detection Kit with 7-amino-actinomycin D (7-AAD) was bought from BioLegend Inc. (San Diego, CA, USA).

### 2.3. Images of the Cells

A digital microscope camera PAXcam2+ (Midwest Information Systems, Inc., Villa Park, IL, USA) adapted with an inverted microscope CKX31 (Olympus Co., Tokyo, Japan) was used to take the images of cell cultures in Figure 1A (at 10× objective lens magnification).

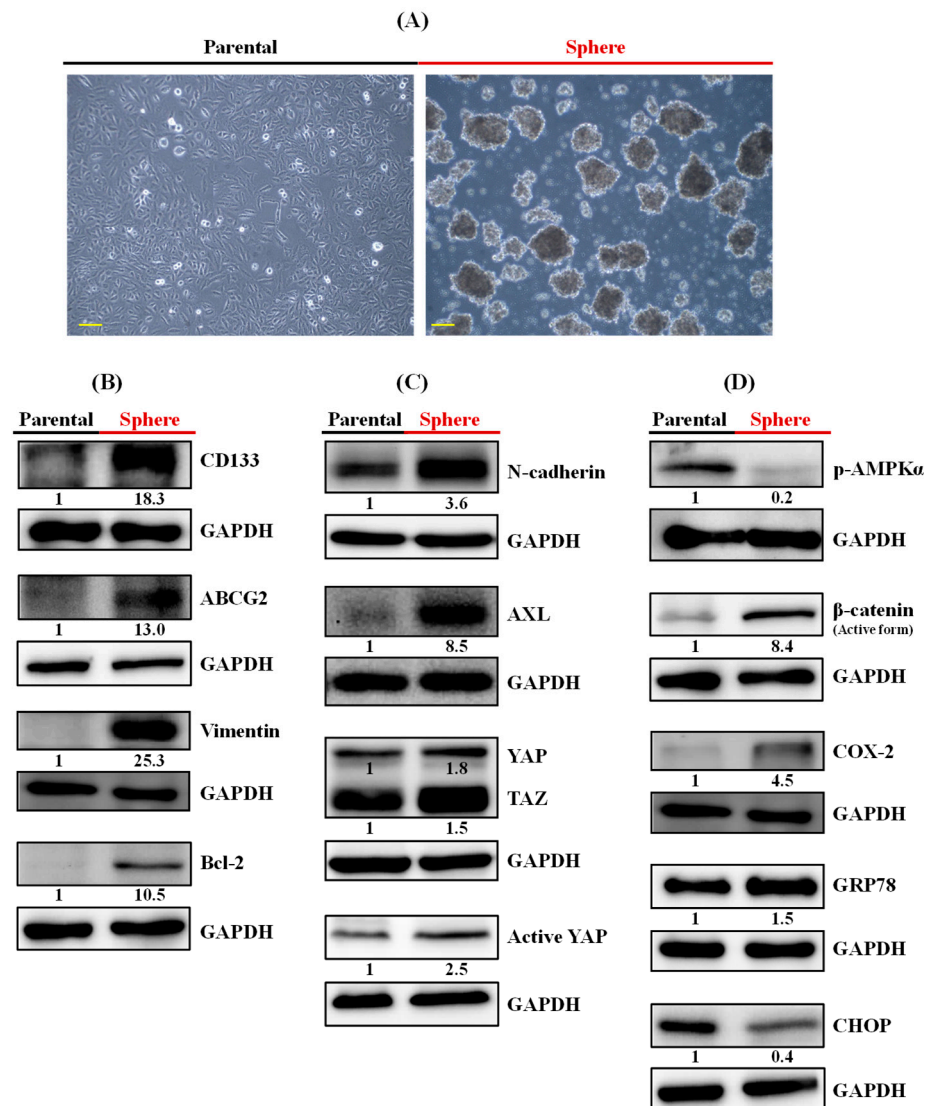


**Figure 1.** Floating A549 sphere cells have reduced AMPK activity and elevated markers of CSC and EMT than parental A549 cells. (A) Morphologies of adherent parental A549 cells and floating A549 sphere cells after 7 days of culture. Scale bar = 100  $\mu$ m. Protein levels of (B) CSC (CD133 and ABCG2) and EMT (vimentin) markers, anti-apoptotic protein Bcl-2, (C) EMT markers (N-cadherin and AXL), oncogenic drivers (active YAP, YAP, and TAZ), (D) reported targets of selenium (p-AMPK,  $\beta$ -catenin, and COX-2), and ER stress-response elements (GRP78 and CHOP) in parental A549 cells and A549 sphere cells. Whole-cell lysates were subjected to Western blot analysis for the proteins of interest, with glyceraldehyde-3-phosphate dehydrogenase (GAPDH) employed as a loading control. The numbers under the bands indicate the relative densitometric ratios to the bands of the loading control. AMPK, AMP-activated protein kinase; CSC, cancer stem cell; Bcl-2, B-cell lymphoma 2; EMT, epithelial-mesenchymal transition; AXL, anexelextko; YAP, yes-associated protein; TAZ, PDZ-binding motif; p-AMPK, phosphorylated AMPK; COX-2, cyclooxygenase-2; ER, endoplasmic reticulum; CHOP, proapoptotic CCAAT/enhancer-binding protein homologous protein; p-AMPK $\alpha$ , phosphorylated AMPK alpha.

#### 2.4. Colony Formation Assay

A549 cells and cultivated A549 sphere cells were plated at density of 150 cells/well in 6-well plate (353046, Falcon, Corning, NY, USA) with RPMI-1640 medium. The formation of colonies was photographed after 7 days of culture. Crystal violet (2%) (C0775, Sigma-Aldrich, Merck KGaA, Darmstadt, Germany) dissolved in 20% methanol solution was used to fix and stain the colonies.

### 2.5. Side Population Detection by DyeCycle Violet (DCV) Exclusion

Twenty four hours after being plated in 10 cm dish ( $3 \times 10^5$  parental A549 cells/dish,  $1 \times 10^6$  A549 sphere cells/dish), agents were added to cells as described in the figure legends. After treatment, cells were harvested from the culture dish, washed twice with phosphate-buffered saline (PBS), and resuspended at a concentration of  $1 \times 10^6$  cells/mL in culture medium at 37 °C (parental A549 in RPMI-1640 and A549 sphere in PluriSTEM™ human ES/iPS cell medium). While protected from light, these cells (1 mL,  $1 \times 10^6$ ) were then incubated for 90 min at 37 °C with either 1 µL (final stain concentration is 5 µM) of DCV alone or in combination with verapamil or reserpine as depicted in the figures. Subsequently, cells were centrifuged immediately for 5 min at  $240 \times g$  and 4 °C, and then resuspended in ice-cold PBS. Propidium iodide (final concentration of 50 µg/mL) was then added to discriminate dead cells. The cells were then kept at 4 °C until subjected to flow cytometric analysis at an excitation of 405 nm and emissions of 450 and 660 nm using a CytoFLEX flow cytometer (Beckman Coulter, Inc., Indianapolis, IN, USA). The gating of side population was confirmed by reserpine and verapamil (ATP-binding cassette (ABC) transporter inhibitors), as indicated.

### 2.6. Apoptotic and Necrotic Cell Death Detected by Annexin V/7-Amino-Actinomycin D Double Staining

After being plated in a 10 cm dish ( $3 \times 10^5$  parental A549 cells/dish,  $1 \times 10^6$  A549 sphere cells/dish) for 24 hours, cells were treated with agents as depicted in the figures for 3 days. Apoptosis and necrosis induction in treated cells were examined by double staining of annexin V and 7-amino-actinomycin D (7-AAD). Double staining with annexin V and 7-AAD is commonly used to discriminate early apoptosis from late apoptosis and necrosis. In early apoptotic stages, cells can exclude the vital dyes, such as 7-AAD (DNA intercalator) because they still maintain the plasma membrane integrity, whereas the phosphatidylserines (PS) on the outer leaflet of the plasma membrane will be stained by annexin V labeled with fluorescein. In contrast, late apoptotic and necrotic cells can be stained by 7-AAD as they lose cell membrane integrity [31]. At harvest, cold Cell Staining Buffer (BioLegend, Inc., San Diego, CA, USA) was used to wash the cells twice, and they were resuspended in Annexin V Binding Buffer (BioLegend, Inc., San Diego, CA, USA) at a density of  $1.6 \times 10^6$  cells/mL. First, 100 µL of the cell suspension was transferred to a 5 mL test tube and then 5 µL of FITC Annexin V (BioLegend, Inc., San Diego, CA, USA) and 5 µL of 7-AAD Viability Staining Solution (BioLegend, Inc., San Diego, CA, USA) were added. After being gently vortexed and incubated for 15 min at room temperature (25 °C) while protected from light, 400 µL of Annexin V Binding Buffer (BioLegend, Inc., San Diego, CA, USA) was added to the tube and then the cells were subjected to flow cytometric analysis by CytoFLEX (Beckman Coulter, Inc., Indianapolis, IN, USA). At least ten thousand events were collected and analyzed.

### 2.7. Measurement of Apoptotic Sub-G1 Fraction

Twenty-four hours after being cultured in 10-cm dish ( $3 \times 10^5$  parental A549 cells/dish,  $1 \times 10^6$  A549 sphere cells/dish), cells were treated with agents as depicted in the figure legends. After treatment, the cells were centrifuged. The cell pellets were reacted with 500 µL (2 µg/mL) of DAPI (4',6-diamidino-2-phenylindole) solution (NPE 731085, Beckman Coulter, Fullerton, USA) in a 1.5 mL Eppendorf tube on ice and then the cell-cycle distribution and apoptotic sub-G1 percentage were measured by a CytoFLEX flow cytometer (Beckman Coulter, Inc., Indianapolis, IN, USA). At least ten thousand events were collected and analyzed.

### 2.8. Western Blot

After being cultured in a 10 cm dish ( $3 \times 10^5$  parental A549 cells/dish,  $1 \times 10^6$  A549 sphere cells/dish) for one day, cells were then treated with agents as depicted in the figures. After treatment, the whole-cell lysates were extracted with  $1 \times$  radioimmunoprecipita-

tion lysis buffer (Merck Millipore, Billerica, MA, USA) containing 1× serine/threonine phosphatase inhibitor cocktail (FC0030-0001, BIONOVAS, Toronto, ON, Canada), 1× tyrosine phosphatase inhibitor cocktail (FC0020-0001, BIONOVAS, Toronto, ON, Canada), and 1× protease inhibitor cocktail, full range (FC0070-0001, BIONOVAS, Toronto, ON, Canada). The protein extracts were separated by sodium dodecyl sulfate–polyacrylamide gel electrophoresis (SDS–PAGE) and then transferred to polyvinylidene difluoride (PVDF) membrane (GE Healthcare, Pittsburgh, PA, USA) by electroblotting. The membranes were blocked by bovine serum albumin (5%) in Tris-buffered saline (TBS) buffer (Tris-buffered saline with Tween 20, 25 mM Tris–hydrochloric acid (HCl), 125 mM sodium chloride (NaCl), 0.1% Tween 20) at room temperature for 1 h and incubated with primary antibody at 4 °C overnight and then with secondary antibody (horseradish peroxidase-conjugated) at room temperature for 1 h. After each incubation period, the membrane was intensively washed with TBS buffer. Finally, the target proteins of the primary antibodies were visualized using enhanced chemiluminescence (ECL) Reagent Plus (Perkin Elmer, Inc., Waltham, MA, USA) on the Syngene G:Box chemi XL gel documentation system (Syngene, Cambridge, UK) according to the manufacturer’s instructions. The intensities of Western blot bands were quantified by using ImageJ software (ImageJ Version 1.52, National Institutes of Health, Bethesda, MD, USA) downloaded from <https://imagej.nih.gov/ij/download.html> (accessed on 25 September 2019).

### 2.9. Antibodies

Primary antibodies against non-phospho (active)  $\beta$ -catenin (Ser33/37/Thr41, #8814), ABCG2 (#4477), phospho-AMPK $\alpha$  (Thr172, #2535), AXL (#8661), TAZ (#8418), active caspase-4 (#4450), full-length caspase-8 (#9746), cleaved caspase-3 (Asp175, #9664), and cleaved caspase-9 (Asp315, #9505) were purchased from Cell Signaling Technology, Inc. (Danvers, MA, USA). Primary antibodies for CHOP (ab11419), GRP78 (ab108613), COX-2 (Ab62331), CD133 (ab19898), vimentin (ab16700), N-cadherin (ab76011), YAP (ab52771), Active YAP (ab205270), Bcl-2 (ab32124), and glyceraldehyde-3-phosphate dehydrogenase (GAPDH) (Ab8245) were bought from Abcam, Inc. (Cambridge, MA, USA).

### 2.10. Cell Viability Measurement

The A549 sphere cells were plated (2000 cells/well) in 96-well culture plates (167008, Thermo Fisher Scientific, Nunc, Waltham, MA, USA) with RPMI-1640 medium for 24 h and then treated with agents indicated in the figures for 3 days. SRB binding assay was used to measure the cell viability. In brief, the cells were fixed by trichloroacetic acid (10%) and incubated for 1 h at 4 °C. Then, the plates were washed with tap water twice and dried in air. The dried plates were stained with 80  $\mu$ L of 0.4% (*w/v*) SRB prepared in 1% (*v/v*) acetic acid at room temperature for 30 min. The unbound SRB in plates was removed by two quick rinses with 1% acetic acid, and the plates were then dried in air until no moisture was apparent. Finally, 20 mmol/L Tris base (200  $\mu$ L/well) was added to dissolve the bound dye on a shaker for 5 min. Optical density at 570 nm was read by a microplate reader ELx800 (BioTek Instruments, Inc., Winooski, VT, USA). The optical density is directly proportional to the viable number of cells over a wide range.

### 2.11. Analysis of Synergistic Combination Effect

The synergistic effect between two treatments on the cell viability of sphere cells was evaluated by the mutually non-exclusive combination index (CI) calculated from the median effect principle of Chou and Talalay [32], using the CalcuSyn software (version 1.1.1; Biosoft, Cambridge, UK). A value of CI = 1 means an additive effect, whereas values of CI < 1 or CI > 1 mean synergistic or antagonistic effect, respectively.

### 3. Results

#### 3.1. CSC-like A549 Sphere Cells Possessed Elevated GRP78 and Reduced CHOP and AMPK Activity

After culture in a defined small-molecule-based serum-free medium in a nonadhesive culture system, floating spheres with round and smooth contours were successfully obtained from A549 (EGFR wild-type, KRAS-G12S) human lung adenocarcinoma cells (Figure 1A). To characterize their stemness, the expression of lung CSC markers, such as CD133 [2] and ABCG2 [33], was examined. Consistent with the previously reported culture of sphere-growing lung cancer cells [34], these A549 sphere cells were highly enriched for CD133 than parental A549 cells (Figure 1B). Consistent with enriched CD133+ cells from human lung cancer cell lines [2], coexpression of elevated ABCG2 was observed in these spheres (Figure 1B). Besides ABCG2, the level of another chemoresistance driver, B-cell lymphoma-2 (Bcl-2) [35], in these sphere cells was also higher than in parental cells (Figure 1B). In accordance with the functional and mechanistic links between EMT and cancer stemness [36], the levels of EMT markers such as vimentin, N-cadherin, and AXL [37] were higher in sphere cells (Figure 1B,C). Moreover, the CSC traits of these sphere cells were further characterized by the elevated YAP and TAZ oncogenic driver levels (Figure 1C). Next, this study examined the reported targets of selenium (AMPK,  $\beta$ -catenin, and COX-2) [38,39] and the ER stress-response elements (GRP78 and CHOP) that could be synergistically regulated by the Se-Y and FO combination as reported in previous studies [16,21]. As shown in Figure 1D, A549 sphere cells have significantly lower AMPK activity and CHOP levels than parental cells and higher levels of  $\beta$ -catenin, COX-2, and GRP78. These molecular features are paradoxical to the combined effects of Se-Y and FO in previous studies [16,21], implying the potential utility of this nutrient combination to counteract these molecular features, accompanied by diminishing the aforementioned CSC traits and cisplatin resistance.

A549 sphere cells were analyzed for clonogenicity, side population proportion, and cisplatin resistance. Consistent with the reported proliferation capability of sphere cells from A549 cells [28], A549 sphere cells in this study formed a larger and higher number of colonies than parental A549 cells after culture for 7 days (Figure 2A). Similar to the elevated ABCG2, the side population percentage increased from 3.57% in parental cells to 19.4% in sphere cells (Figure 2B).

When cells were treated with cisplatin (20  $\mu$ g/mL) for 72 h, the apoptotic sub-G1 fraction in parental A549 cells was markedly increased, from 1.64% to 24.77% (Figure 2C, top). In contrast, the sub-G1 fraction in floating A549 sphere cells only slightly increased, from 8.58% to 10.1%, at the same concentration of cisplatin (Figure 2C, middle). After treating A549 sphere cells with cisplatin (20  $\mu$ g/mL) in the same serum containing culture condition as parental cells, the sub-G1 fraction still slightly increased from 6.13% to 8.19% (Figure 2C, bottom). The cell cycle distribution of these cisplatin (20  $\mu$ g/mL)-treated cells is described in Table 1. This phenomenon was further confirmed by the annexin V/7-AAD double staining assay that revealed compatible percentages of early apoptosis (lower right quadrant), late apoptosis (upper right quadrant), and necrosis (upper left quadrant) of cells (Figure 2D) treated as that in Figure 2C. Compared to parental cells, A549 sphere cells were relatively resistant to cisplatin-induced cell death.

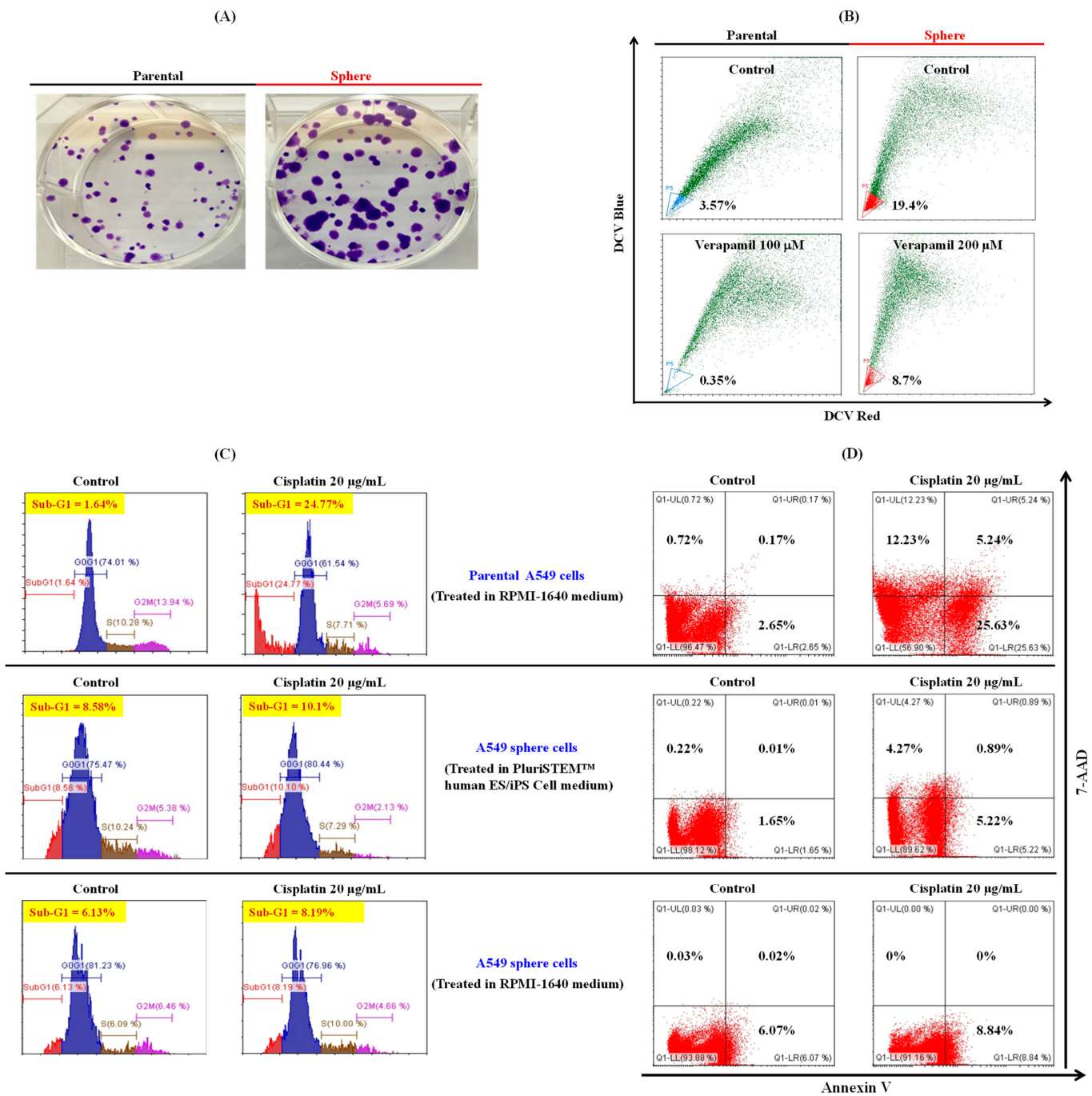


**Figure 2.** A549 sphere cells have higher clonogenicity, side population proportion, and resistance to cisplatin-induced apoptosis. **(A)** Colony formation of parental A549 cells and A549 sphere cells after 7 days of culture in the same medium (RPMI-1640), as described in Materials and Methods section. **(B)** Side population percentage analyzed by DyeCycle Violet (DCV) staining and flow cytometry. The side population percentage is indicated in the lower left side of each flow cytometry dot plot. ATP-binding cassette (ABC) transporter inhibitor verapamil was employed to conform the gating of side population, as indicated. **(C)** Percentage of apoptotic sub-G1 fractions of parental A549 (top), A549 sphere cells in PluriSTEM™ medium (middle), and A549 sphere cells in RPMI-1640 medium (bottom) after treatment with 20 µg/mL cisplatin for 72 h. **(D)** The percentages of early apoptotic (lower right quadrant, Q1-LR), late apoptotic (upper right quadrant, Q1-UR), necrotic (upper left quadrant, Q1-UL), and viable (lower left quadrant, Q1-LL) cells analyzed by annexin V/7-AAD double staining and flow cytometry. The cells were grouped and treated as described in (C). Sub-G1 (SubG1), G0G1, S, and G2M mean Cell-cycle phase distribution. 7-AAD, 7-amino-actinomycin D.



**Table 1.** Cell-cycle phase distribution (%) of 72 h cisplatin-treated parental A549 and A549 sphere cells in Figure 2C.

	Treatment	Cell-Cycle Distribution			
		Sub-G1 (%)	G1 (%)	S (%)	G2/M (%)
Parental A549	Control	1.64	74.01	10.28	13.94
Parental A549	Cisplatin 20 µg/mL	24.77	61.54	7.71	5.69
A549 sphere (in PluriSTEM™)	Control	8.58	75.47	10.24	5.38
A549 sphere (in PluriSTEM™)	Cisplatin 20 µg/mL	10.1	80.44	7.29	2.13
A549 sphere (in RPMI-1640)	Control	6.13	81.23	6.09	6.46
A549 sphere (in RPMI-1640)	Cisplatin 20 µg/mL	8.19	76.96	10	4.66

### 3.2. Se-Y and FO Synergistically Induced Apoptosis of A549 Sphere Cells and Diminished CSC Traits

This study assessed the combined effects of Se-Y and FO on cisplatin-resistant A549 sphere cells. Consistent with a previous study [16], the combination of Se-Y (200 ng/mL) and FO (200 µM) induced the apoptotic sub-G1 fraction from 1.9% in the control group to 42.2%, whereas individual treatment only slightly increased the apoptotic fraction, to 14.4% and 3.4%, respectively (Figure 3A). The combined effects of Se-Y and FO on the cell-cycle distribution of A549 sphere cells are listed in Table 2. This result was further confirmed by the annexin V/7-AAD double staining assay, which showed compatible percentages of early apoptosis (lower right quadrant), late apoptosis (upper right quadrant) and necrosis (upper left quadrant) of A549 sphere cells (Figure 3B) treated as that in Figure 3A. Accordingly, the cell viability assay showed that combination of Se-Y (200 ng/mL) and FO (200 µM) suppressed the viability of A549 sphere cells to 27.3% of control, whereas individual treatment only slightly reduced the cell viability to 70.3% and 77.9% of control, respectively (Figure 3C). Evaluating the synergism of this combination by combination index (CI), most of the CI values were all below 1 (synergistic effect), except a value of 1.078 (Table 3). Further, the combined effects on ER stress-response elements (CHOP and GRP78) and the reported targets of selenium ( $\beta$ -catenin and COX-2) [38,39] were examined. Although the individual effects of Se-Y (200 ng/mL) and FO (200 µM) were relatively mild, the combination of these nutrients not only reduced the elevated pro-survival GRP78 level, but also drastically increased the pro-apoptotic CHOP of A549 sphere cells (Figure 3D), along with marked activation of caspase-3, the terminal executioner of apoptosis (Figure 3E). A similar pattern of the combined effects on reducing  $\beta$ -catenin and COX-2 was also observed in A549 sphere cells treated with the Se-Y and FO combination (Figure 3D). In agreement with the pro-apoptotic modulation of GRP78 and CHOP (Figure 3D), ER stress-related caspase-4 [40] in A549 sphere cells was synergistically activated by the combination of Se-Y and FO (Figure 3E). Similar effects were also observed on caspase-9 induction, anti-apoptotic Bcl-2 suppression, and full-length caspase-8 cleavage (Figure 3E).

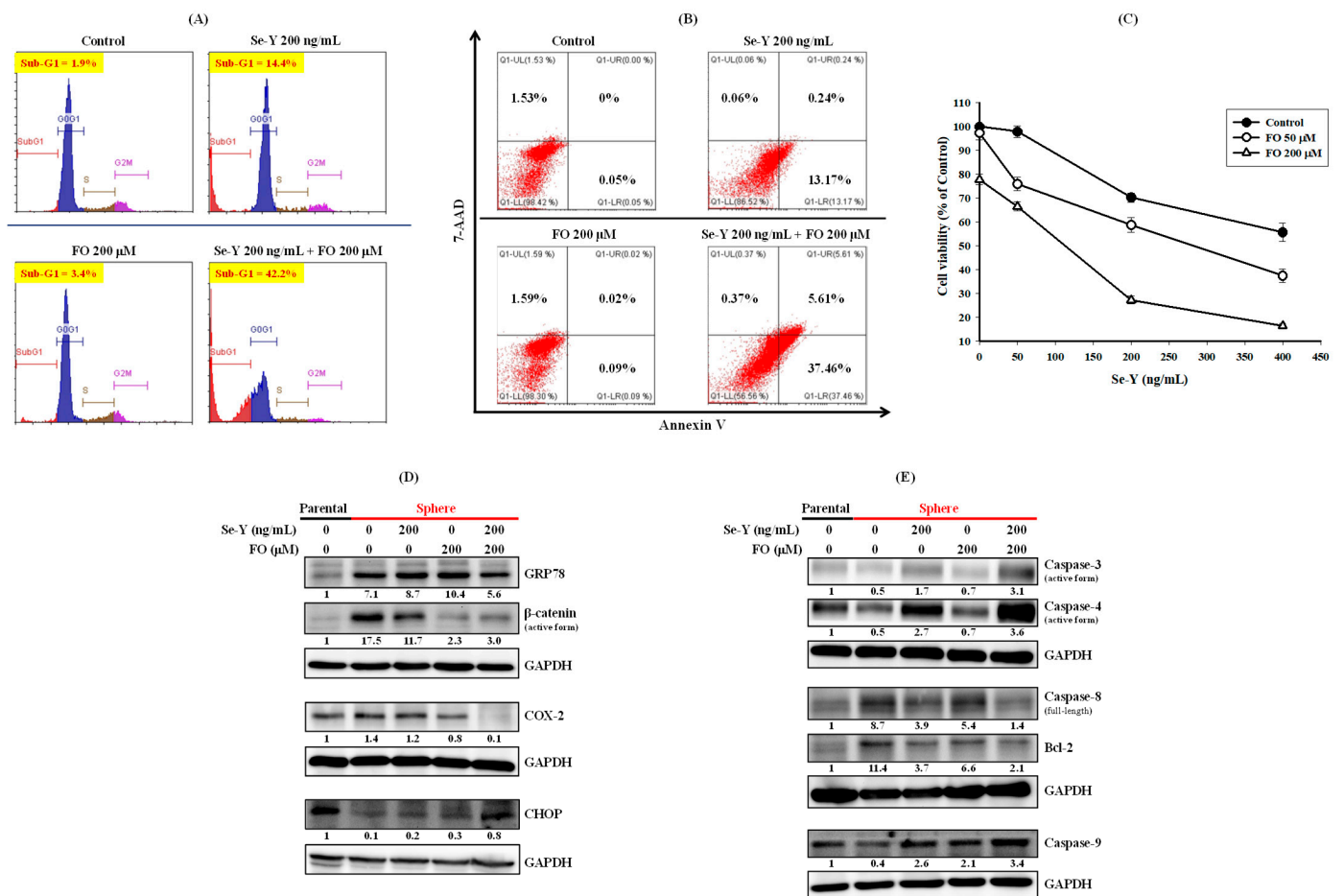


**Figure 3.** Selenium yeast (Se-Y) and fish oil (FO) combination synergistically induced apoptosis, suppressed cell viability, and modulated ER stress-response elements of A549 sphere cells. (A) The apoptotic sub-G1 percentage of A549 sphere cells after treatment with Se-Y, FO alone or in combination for 72 h. (B) The percentages of early apoptotic (lower right quadrant, Q1-LR), late apoptotic (upper right quadrant, Q1-UR), necrotic (upper left quadrant, Q1-UL), and viable (lower left quadrant, Q1-LL) A549 sphere cells analyzed by annexin V/7-AAD double staining and flow cytometer. (C) Combined effect of Se-Y and FO on the viability (mean ± standard error) of A549 sphere cells after 72 h of treatment (performed in RPMI-1640 medium as described in Materials and Methods section). Combined effects of Se-Y and FO on the protein levels of (D) ER stress-response elements (GRP78 and CHOP), COX-2, activated β-catenin, (E) caspase-3, 4, 9, full-length caspase-8, and Bcl-2 of A549 sphere cells after 72 h of treatment. Whole-cell lysates were subjected to Western blot analysis for the proteins of interest, employing glyceraldehyde-3-phosphate dehydrogenase (GAPDH) as a loading control. The numbers under the bands indicate the relative densitometric ratios to the bands of the loading control.

**Table 2.** Cell-cycle phase distribution (%) of A549 sphere cells treated with selenium yeast (Se-Y) alone, fish oil (FO) alone, or in combination for 72 h in Figure 3A.

A549 Sphere Cells	Cell-Cycle Distribution				
	Treatment	Sub-G1 (%)	G1 (%)	S (%)	G2/M (%)
Control		1.9	80.9	7.8	9.4
Se-Y 200 ng/mL		14.4	73.3	4.8	7.5
FO 200 μM		3.4	78.9	9.9	7.8
Se-Y 200 ng/mL + FO 200 μM		42.2	48.5	5.9	3.4

**Table 3.** Combination index (CI) values of selenium yeast (Se-Y) and fish oil (FO) combinations vs. the suppression (FA, fraction affected) on viability of A549 sphere cells. The concentration of FO represents its content of omega-3 fatty acids (DHA + EPA). Values below 1 indicate synergistic effects; those equal or close to 1 are additive, and those above 1 are antagonistic.

Se-Y (ng/mL)	FO ( $\mu$ M)	FA (0–1)	CI
50	50	0.368	0.389
50	200	0.334	1.078
200	50	0.412	0.941
200	200	0.727	0.645
400	50	0.624	0.968
400	200	0.835	0.656

DHA, docosahexaenoic acid; EPA, eicosapentaenoic acid.

The protein levels of lung CSC markers, such as CD133 [2] and ABCG2 [33], were examined to determine whether this synergistic apoptosis induction was accompanied by the suppression of CSC traits. As expected, elevated ABCG2 and CD133 in A549 sphere cells were suppressed by the Se-Y and FO combination (Figure 4A). In agreement with its reported effect on AMPK activation [16], this combination increased AMPK activity upon suppressing ABCG2 in A549 sphere cells (Figure 4A). Additionally, elevated EMT markers (vimentin, AXL, and N-cadherin) and oncogenic drivers conferring CSC traits (active YAP, YAP, and its paralog TAZ) were all suppressed by the Se-Y and FO combination in a similar manner (Figure 4B). The combination of Se-Y and FO not only induced apoptosis, but also diminished CSC traits and EMT markers of cisplatin-resistant A549 sphere cells.

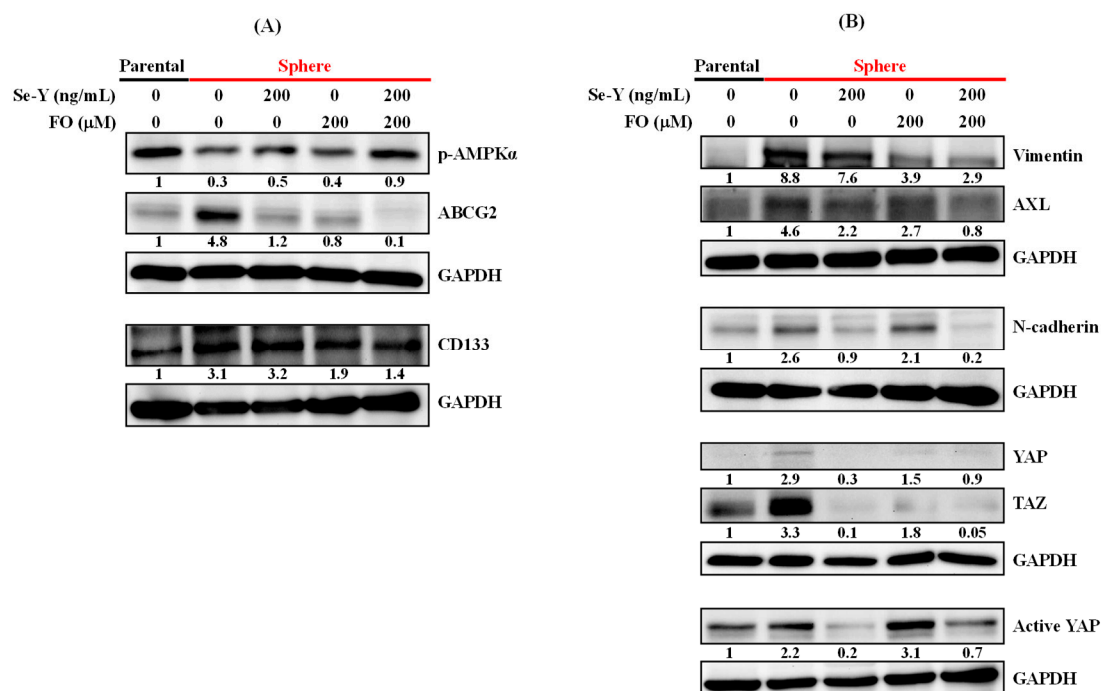


**Figure 4.** Selenium yeast (Se-Y) and fish oil (FO) combination synergistically activated AMPK and diminished CSC and EMT markers in A549 sphere cells. Combined effects of Se-Y and FO on the protein levels of (A) activated AMPK (p-AMPK $\alpha$ ), CSC markers (ABCG2 and CD133), (B) EMT markers (vimentin, AXL, and N-cadherin), and oncogenic drivers (active YAP, YAP, and TAZ) in A549 sphere cells after treatment with Se-Y alone, FO alone, or in combination for 72 h. Whole-cell lysates were subjected to Western blot analysis for the proteins of interest, employing glyceraldehyde-3-phosphate dehydrogenase (GAPDH) as a loading control. The numbers under the bands indicate the relative densitometric ratios to the bands of the loading control.

### 3.3. Se-Y and FO Combination Suppressed the Side Population of A549 Sphere Cells Via AMPK Activation

AMPK activation suppressed ABCG2 in A549 cells and thus decreased the side population percentage [7]. Subsequently, the side population percentage in A549 sphere cells was analyzed after AMPK modulation by the Se-Y and FO combination or AMPK inhibitor compound C (dorsomorphin). In Figure 5A, AMPK activation by the Se-Y and FO combination was eliminated when sphere cells were pretreated with compound C for 1 h and washed out. In line with the modulation of AMPK activity, the side population percentage was reduced from 16.1% in control sphere cells to 5.9% by the combination of Se-Y and FO (Figure 5B); in contrast, in sphere cells pretreated with compound C for 1 h and washed, the side population was only reduced to 11.5% by the combination of Se-Y and FO (Figure 5B). There was a negative reciprocal interplay between AMPK and the side population proportion in A549 sphere cells.

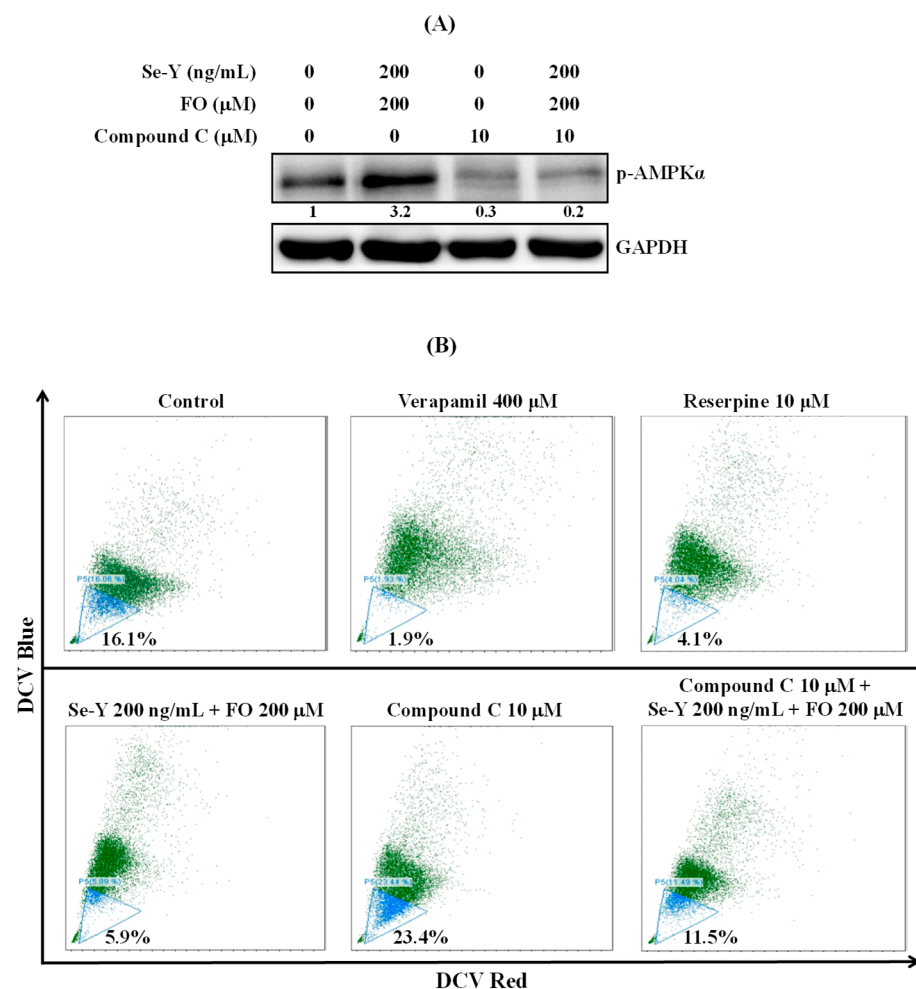


**Figure 5.** Selenium yeast (Se-Y) and fish oil (FO) combination suppressed the side population in A549 sphere cells via AMPK activation. The AMPK inhibitor (compound C) was pretreated for 1 h and washed out before adding Se-Y and FO. (A) Combination effect of Se-Y and FO on the AMPK activity of A549 sphere cells after 72 h of treatment with or without pretreatment with AMPK inhibitor (compound C) for 1 h. (B) Side population percentage analyzed by DyeCycle Violet (DCV) staining and flow cytometry. The side population percentage is indicated in the lower left side of each flow cytometry dot plot. ATP-binding cassette (ABC) transporter inhibitors reserpine and verapamil were employed to conform the gating of side population, as depicted. A549 sphere cells were treated with combination of Se-Y and FO for 72 h with or without pretreatment with AMPK inhibitor (compound C) for 1 h.

### 3.4. Se-Y and FO Combination Reversed Cisplatin Resistance in A549 Sphere Cells

In addition to inducing the side population phenotype [7], the efflux molecule ABCG2 also contributes to A549 cell resistance to cisplatin [22,23,41]. Given the substantial decrease of ABCG2 in this nutrient combination-treated A549 sphere cells, their cisplatin sensitivity was analyzed. As expected, cisplatin (20 µg/mL) did not substantially increase the apoptotic sub-G1 fraction (9.37% to 8.34%) in A549 sphere cells after 72 h of treatment (Figure 6A). However, cisplatin (20 µg/mL) further increased the sub-G1 fraction in Se-Y (200 ng/mL) and FO (200 µM) combination-treated sphere cells from 45.87% to 63.02% (Figure 6A). The Se-Y and FO combination at half the concentrations in Figure 6A elevated the sub-G1 fraction of A549 sphere cells from 8.46% to 37.77%. This apoptotic fraction could be further enhanced to 71.58% by cisplatin (20 µg/mL; Figure 6B). These data indicate that combining Se-Y and FO restored A549 sphere cell sensitivity to cisplatin. Tables 4 and 5 list the cell-cycle distribution of A549 sphere cells described in Figure 6A,B, respectively. The results in Figure 6B were further confirmed by the annexin V/7-AAD double staining assay showing compatible percentages of early apoptosis (lower right quadrant), late apoptosis (upper right quadrant), and necrosis (upper left quadrant) of A549 sphere cells (Figure 6C) treated as in Figure 6B. In the presence of the Se-Y and FO combination, A549 sphere cell resistance to cisplatin was reversed. A similar result was also obtained by the cell viability test determined by sulforhodamine B staining. As shown in Figure 6D, the effect of cisplatin on the cell viability of A549 sphere cells was enhanced by the combination of Se-Y and FO. When evaluating the synergism by CI, the CI values of the combination of cisplatin with Se-Y and FO were all below 1 (Table 6), which indicates synergistic effect.

**Table 4.** Cell-cycle phase distribution (%) of A549 sphere cells treated with cisplatin (20 µg/mL) alone or in combination of selenium yeast (Se-Y) and fish oil (FO) for 72 h in Figure 6A.

A549 Sphere Treatment	Cell-Cycle Distribution			
	Sub-G1 (%)	G1 (%)	S (%)	G2/M (%)
Control	9.37	67.53	15.32	6.43
Se-Y 200 ng/mL + FO 200 µM	45.87	44.15	6.44	2.43
Cisplatin 20 µg/mL	8.34	62.82	17.77	7.61
Cisplatin 20 µg/mL + Se-Y 200 ng/mL + FO 200 µM	63.02	24.53	5.58	2.67

**Table 5.** Cell-cycle phase distribution (%) of A549 sphere cells treated with cisplatin (20 µg/mL) alone or in combination of selenium yeast (Se-Y) and fish oil (FO) for 72 h in Figure 6B.

A549 Sphere Treatment	Cell-Cycle Distribution			
	Sub-G1 (%)	G1 (%)	S (%)	G2/M (%)
Control	8.46	73.9	6.84	10.28
Se-Y 100 ng/mL + FO 100 µM	37.77	47.48	7.66	6.09
Cisplatin 20 µg/mL	5.28	80.95	8.06	5.1
Cisplatin 20 µg/mL + Se-Y 100 ng/mL + FO 100 µM	71.58	22.13	4.51	0.82

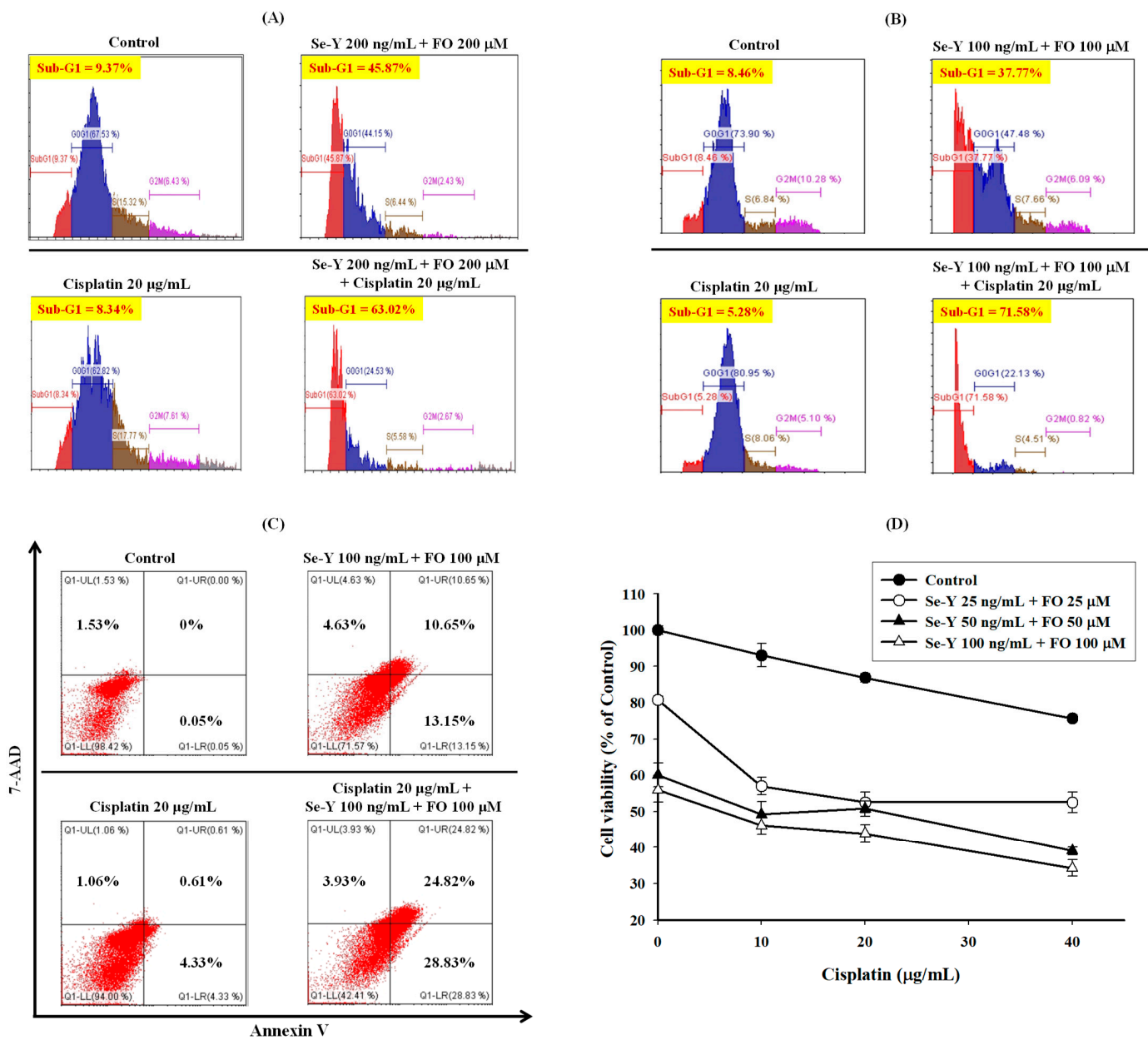


**Figure 6.** Selenium yeast (Se-Y) and fish oil (FO) combination reversed the resistance of A549 sphere cells to cisplatin. (A) The apoptotic sub-G1 percentage of A549 sphere cells after treatment with cisplatin (20 μg/mL) alone or in combination with Se-Y (200 ng/mL) and FO (200 μM) for 72 h. (B) The apoptotic sub-G1 percentage of A549 sphere cells after treatment with cisplatin (20 μg/mL) alone or in combination of Se-Y (100 ng/mL) and FO (100 μM) for 72 h. (C) The percentages of early apoptotic (lower right quadrant, Q1-LR), late apoptotic (upper right quadrant, Q1-UR), necrotic (upper left quadrant, Q1-UL), and viable (lower left quadrant, Q1-LL) A549 sphere cells analyzed by annexin V/7-AAD double staining and flow cytometry. The cells were subjected to annexin V/7-AAD double staining assay together with that in Figure 3B and compared to the same control. (D) The viability of A549 sphere cells treated with cisplatin alone or in combination with Se-Y and FO in RPMI-1640 medium as described in Materials and Methods section for 72 h. Data are expressed as mean ± standard error.

**Table 6.** Combination index (CI) values of combining cisplatin with selenium yeast (Se-Y) and fish oil (FO) vs. the suppression (FA, fraction affected) on viability of A549 sphere cells. The concentration of FO represents its content of omega-3 fatty acids (DHA + EPA). Values below 1 indicate synergistic effects; those equal or close to 1 are additive, and those above 1 are antagonistic.

Cisplatin ( $\mu\text{g/mL}$ )	Se-Y (ng/mL)	FO ( $\mu\text{M}$ )	FA (0–1)	CI
10	25	25	0.43	0.456
10	50	50	0.508	0.548
10	100	100	0.539	0.875
20	25	25	0.474	0.486
20	50	50	0.492	0.721
20	100	100	0.561	0.898
40	25	25	0.474	0.721
40	50	50	0.61	0.549
40	100	100	0.658	0.68

#### 4. Discussion

Cisplatin resistance remains a serious unresolved clinical and scientific challenge in lung cancer treatment. Apart from the tyrosine kinase inhibitor (TKI)-responsive population, NSCLC patients without mutations for targeted therapies remain heavily reliant on conventional chemotherapy, in which cisplatin is primarily used. Although a successful initial response is achieved in some patients, drug resistance eventually develops in all lung cancers [28]. Cisplatin resistance was detected in 1409 (63%) of 2227 NSCLC clinical cell cultures, which may account for the marginal survival advantage after empiric adjuvant chemotherapy for resected NSCLC [42]. Only a minor portion of NSCLC patients have an improved survival advantage after adjuvant chemotherapy, and most endure toxicity without acquiring benefits [42]. Thus far, no clinically available drug can overcome cisplatin resistance or kill cisplatin-resistant cells [43]. Novel therapeutics or alternative strategies are pressingly needed. This study demonstrated the synergistic effects of combining Se-Y and FO on apoptosis induction in cisplatin-resistant A549 sphere cells, accompanied by diminishing CD133 and ABCG2, two important therapeutic targets for relieving the cisplatin resistance of NSCLC. CD133 protein expression tended to correlate with a shorter median progression-free survival and early recurrence in stage IIIB/IV NSCLC patients treated with platinum-containing regimens [6]. ABCG2 overexpression confers the side population phenotype, which is employed for quantifying the chemoresistant subpopulation in cancer cells [7]. ABCG2 inhibition resensitized NSCLC to cisplatin [22,41]. Accordingly, CD133+ABCG2+ subpopulation cells could be spared from cisplatin treatment in mice xenografts established from human primary lung cancers [6]. In agreement with mentioned above, substantial inhibition of ABCG2 and CD133 in A549 sphere cells by the Se-Y and FO combination resulted in a smaller side population and cisplatin resistance.

There was a negative reciprocal relationship between AMPK activity and the side population percentage of parental and sphere-forming populations of A549 cells, and the Se-Y and FO combination could activate AMPK to reduce the side population of A549 sphere cells. Liu et al. demonstrated that increasing glucose concentration could suppress AMPK to expand the CSC-like side population in cell lines, including A549 [7]. They demonstrated that cisplatin mainly killed non-side population cells and thus increased the side population and tumor-initiating capacity (in mice) of A549 cells [7]. In contrast, the glycolysis inhibitor 3-bromo-2-oxopropionate-1-propyl ester (3-BrOP) could activate AMPK and reduce the side population in A549 cells, resulting in impaired tumor-initiating capacity in mice [7]. The elimination of the side population appears to be a potentially effective strategy for improving NSCLC treatment. In line with this, combining Se-Y and FO reduced the side population in A549 sphere cells and reversed their cisplatin resistance. In the study conducted by Liu et al., the high-glucose-elevated CSC-like side population [7] might echo studies illustrating that hyperglycemia may contribute to a more malignant phenotype of cancer cells and confer resistance to chemotherapy [44,45]. In addition to diabetes mellitus,

hyperglycemia can occur in obesity, pancreatitis, chronic stress, and cancer [44]. In cancer patients harboring phenotypes as A549 cells and the above co-morbidities, the combination of Se-Y and FO might potentially alleviate hyperglycemia-mediated cancer fostering effects by diminishing the elevated CSC-like side population.

AMPK is an emerging anticancer target [46]. Accordingly, this study and the one by Liu et al. [7] showed a negative reciprocal interaction between AMPK activity and the side population. Thus, metformin, a well-known antidiabetic drug and an AMPK activator, has recently received a surge of interest for its potential as an anticancer agent [46]. Metformin was shown to relieve cisplatin resistance [47], eliminate CSCs [48–50], and provide benefits in cancer prevention and treatment [45,46,49,51]. However, unlike the clinically achievable concentrations of Se-Y and FO [52,53] used in this study, most of the effective anticancer concentrations of metformin employed in preclinical studies were supraphysiological (at the millimolar range) [50,54]. Although metformin penetrated certain tumors and concentrations reaching 100  $\mu$ M were detected in rodents [55], the maximum plasma concentration of metformin in healthy human subjects was only 8–16  $\mu$ M [56]. Considering the combined effects of Se-Y and FO at clinically achievable concentrations, it seemed logical to postulate that combining Se-Y and FO might exert benefits for cancer prevention and treatment similar to metformin, including but not limited to the condition of hyperglycemia.

AMPK inhibits the oncogenic driver YAP and its paralog TAZ, which regulate CSC biology, including drug resistance, EMT [30], ABCG2, and the side population [57]. In agreement, compared to parental A549 cells, AMPK activity was reduced in sphere cells. YAP activity and the related CSC and EMT markers were elevated. Consistent with AMPK activation by the combination of Se-Y and FO, the profound inhibition of YAP activity was displayed in these treated A549 sphere cells, and the features of YAP induction were substantially reversed.

Besides YAP, the aberrant elevation of the cytoprotective ER chaperone GRP78 also promoted the CSC traits, EMT, drug resistance, metastasis, and tumorigenesis of lung cancer cells [58]. Accordingly, elevated GRP78 was observed in CSC-like A549 sphere cells. Their lowered level of proapoptotic ER stress effector CHOP further confirmed their cisplatin resistance. Unlike the simultaneous induction of CHOP and GRP78 by selenium (methylseleninic acid) alone in prostate cancer cells [59], a previous study reported the opposite regulation of CHOP and GRP78 by the combination of Se-Y and FO to induce apoptosis in A549 NSCLC cells via AMPK activation [16]. Consistent with observations in gefitinib-resistant HCC827 NSCLC cells [21], this study further demonstrated CHOP induction along with GRP78 suppression by the Se-Y and FO combination in cisplatin-resistant A549 sphere cells. The ER stress-related caspase-4 [40] in these treated sphere cells was synergistically activated upon massive induction of apoptosis. GRP78 is considered a potential marker for lung cancer diagnosis and prognosis [58]. Besides the above-mentioned AMPK [46] and ABCG2 [6], GRP78 is also an emerging anticancer target for new therapeutic interventions [58]. Targeting cell-surface GRP78 enhanced pancreatic cancer radiosensitivity by inhibiting YAP/TAZ protein signaling [60]. The inhibition of GRP78 and YAP/TAZ by the Se-Y and FO combination suggested its potential radiosensitizing effect in these treated A549 sphere cells. In accordance with this, the nutrition supplement containing Se-Y, EPA, and DHA enhanced the anticancer effects of radiotherapy on lung cancer-bearing mice [61]. The GRP78-suppressing effects of the Se-Y and FO combination in previous studies [16,21] and this study also suggested the potential clinical impact of this nutrient combination in lung cancer therapy.

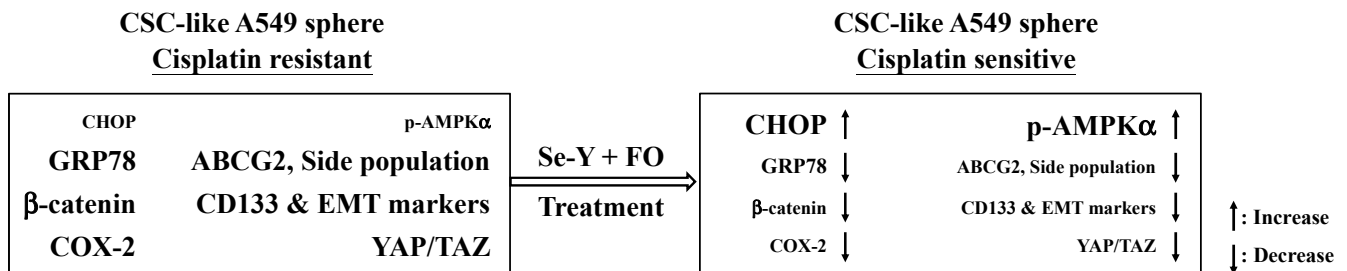
Recent studies supported the notion that AMPK activation enhances the anticancer effects of cisplatin [62,63]. Nevertheless, some studies reported conflicting results on the tumor-promoting effects of AMPK activation [64,65]. Now, it is proposed that AMPK can behave as a CSC “friend” or “foe” in a tissue type-specific and context-dependent manner [65]. The widespread use of AMPK activators should be trialed cautiously across disease settings of cancers [64]. Cancer cells elicit complicated responses that are not fully understood to survive from treatments. Treatment with cisplatin combined with Se-Y and



FO might also lead to a resistant subpopulation characterized by different responses to AMPK activation. Nevertheless, based on this study and the reported tumor-suppressing effects of AMPK activation in A549 cells [7,63], the combination of Se-Y and FO may potentially improve the outcomes of cisplatin-treated NSCLC with phenotypes such as A549 cells and warrant further tests in preclinical mouse models, followed by clinical evaluation.

## 5. Conclusions

Cisplatin is widely prescribed for NSCLC that is difficult to treat by targeted therapy. Studies worldwide have explored therapeutics to overcome NSCLC cisplatin resistance. This study demonstrated that combining Se-Y and FO at clinically achievable concentrations could synergistically induce apoptosis in A549 NSCLC sphere cells, accompanied by a reversal of their cisplatin resistance. As shown in Scheme 1, this nutrient combination induced proapoptotic CHOP, activated AMPK, and suppressed the reported therapeutic targets, such as ABCG2, GRP78, the side population, and YAP/TAZ. Compared to synthetic pharmacologic agents, combining cisplatin with edible dietary nutrients such as Se-Y and FO may offer therapeutic efficacy with minimal or no toxicity to the physiological system. The results suggest potential application of the Se-Y and FO combination to improve the outcomes of cisplatin-treated NSCLC with phenotypes such as A549 cells.



**Scheme 1.** Schematic diagram of the proposed mechanisms of action of the selenium yeast (Se-Y) and fish oil (FO) combination for inducing apoptosis and reversing cisplatin resistance in CSC-like A549 sphere cells. CSC, cancer stem cell; CHOP, proapoptotic CCAAT/enhancer-binding protein homologous protein; COX-2, cyclooxygenase-2; p-AMPK $\alpha$ , phosphorylated AMPK alpha; EMT, epithelial–mesenchymal transition; YAP, yes-associated protein; TAZ, PDZ-binding motif.

**Author Contributions:** Conceptualization, I.-C.L., H.-Y.C. and C.-J.Y.; methodology, C.-H.L. and W.-L.T.; investigation, M.-H.H., C.-L.C. and Y.-Y.L.; execution of experiments, W.-L.T.; resources, S.-E.C. and S.H.; writing—original draft preparation, I.-C.L. and C.-J.Y.; writing—review and editing, H.-Y.C., G.-M.L. and C.-J.Y.; supervision, T.-J.C. and J.W.-P.; project administration, W.-L.T. and C.-J.Y.; funding acquisition, G.-M.L. and C.-J.Y. All authors have read and agreed to the published version of the manuscript.

**Funding:** This research was supported by a research grant from Wan Fang Hospital, Taipei Medical University, Taipei, Taiwan (110-wf-eva-11), joint grant of Wan Fang Hospital, Taipei Medical University and New Health Products Co., Ltd., Taipei, Taiwan (W327-3), and the Ministry of Science and Technology, Taiwan (MOST 110-2320-B-038-068). The APC was funded by New Health Products Co., Ltd., Taipei, Taiwan.

**Institutional Review Board Statement:** Not applicable.

**Informed Consent Statement:** Not applicable.

**Data Availability Statement:** Data are available on request.

**Acknowledgments:** The authors would like to thank Chih-Hung Guo (Institute of Biomedical Nutrition, Hung-Kuang University, Taichung, Taiwan) for providing the selenium yeast and fish oil.

**Conflicts of Interest:** This work was partially supported by a joint grant from Wan Fang Hospital, Taipei Medical University and New Health Products Co., Ltd., Taipei, Taiwan (W327-3). Chih-Jung Yao and Gi-Ming Lai are the Principal Investigator and Co-Principal Investigator of the Grant W327-3, respectively. The funders had no role in the design, interpretation of data, writing of the manuscript, or decision to publish the results.

## References

1. Sung, H.; Ferlay, J.; Siegel, R.L.; Laversanne, M.; Soerjomataram, I.; Jemal, A.; Bray, F. Global Cancer Statistics 2020: GLOBOCAN Estimates of Incidence and Mortality Worldwide for 36 Cancers in 185 Countries. *CA Cancer J. Clin.* **2021**, *71*, 209–249. [[CrossRef](#)] [[PubMed](#)]
2. Cortes-Dericks, L.; Galetta, D. Impact of Cancer Stem Cells and Cancer Stem Cell-Driven Drug Resiliency in Lung Tumor: Options in Sight. *Cancers* **2022**, *14*, 267. [[CrossRef](#)] [[PubMed](#)]
3. Lortet-Tieulent, J.; Soerjomataram, I.; Ferlay, J.; Rutherford, M.; Weiderpass, E.; Bray, F. International trends in lung cancer incidence by histological subtype: Adenocarcinoma stabilizing in men but still increasing in women. *Lung Cancer* **2014**, *84*, 13–22. [[CrossRef](#)] [[PubMed](#)]
4. Gairola, K.; Gururani, S.; Bahuguna, A.; Garia, V.; Pujari, R.; Dubey, S.K. Natural products targeting cancer stem cells: Implications for cancer chemoprevention and therapeutics. *J. Food Biochem.* **2021**, *45*, e13772. [[CrossRef](#)] [[PubMed](#)]
5. Liu, Y.-P.; Yang, C.-J.; Huang, M.-S.; Yeh, C.-T.; Wu, A.T.; Lee, Y.-C.; Lai, T.-C.; Lee, C.-H.; Hsiao, Y.-W.; Lu, J.; et al. Cisplatin Selects for Multidrug-Resistant CD133+ Cells in Lung Adenocarcinoma by Activating Notch Signaling. *Cancer Res.* **2013**, *73*, 406–416. [[CrossRef](#)]
6. Bertolini, G.; Roz, L.; Perego, P.; Tortoreto, M.; Fontanella, E.; Gatti, L.; Pratesi, G.; Fabbri, A.; Andriani, F.; Tinelli, S.; et al. Highly tumorigenic lung cancer CD133+ cells display stem-like features and are spared by cisplatin treatment. *Proc. Natl. Acad. Sci. USA* **2009**, *106*, 16281–16286. [[CrossRef](#)]
7. Liu, P.-P.; Liao, J.; Tang, Z.-J.; Wu, W.-J.; Yang, J.; Zeng, Z.-L.; Hu, Y.; Wang, P.; Ju, H.-Q.; Xu, R.-H.; et al. Metabolic regulation of cancer cell side population by glucose through activation of the Akt pathway. *Cell Death Differ.* **2013**, *21*, 124–135. [[CrossRef](#)]
8. Moselhy, J.; Srinivasan, S.; Ankem, M.K.; Damodaran, C. Natural Products That Target Cancer Stem Cells. *Anticancer Res.* **2015**, *35*, 5773–5788.
9. Burnett, J.; Newman, B.; Sun, D. Targeting cancer stem cells with natural products. *Curr. Drug Targets* **2012**, *13*, 1054–1064. [[CrossRef](#)]
10. Scarpa, E.-S.; Ninfali, P. Phytochemicals as Innovative Therapeutic Tools against Cancer Stem Cells. *Int. J. Mol. Sci.* **2015**, *16*, 15727–15742. [[CrossRef](#)]
11. Naujokat, C. The “Big Five” Phytochemicals Targeting Cancer Stem Cells: Curcumin, EGCG, Sulforaphane, Resveratrol and Genistein. *Curr. Med. Chem.* **2021**, *28*, 4321–4342. [[CrossRef](#)] [[PubMed](#)]
12. Venkateswaran, V.; Klotz, L.H.; Ramani, M.; Sugar, L.M.; Jacob, L.E.; Nam, R.K.; Fleshner, N.E. A Combination of Micronutrients Is Beneficial in Reducing the Incidence of Prostate Cancer and Increasing Survival in the Lady Transgenic Model. *Cancer Prev. Res.* **2009**, *2*, 473–483. [[CrossRef](#)] [[PubMed](#)]
13. Sauter, E.R. Cancer prevention and treatment using combination therapy with natural compounds. *Expert Rev. Clin. Pharmacol.* **2020**, *13*, 265–285. [[CrossRef](#)] [[PubMed](#)]
14. Lu, J.; Zhang, J.; Jiang, C.; Deng, Y.; Özten, N.; Bosland, M.C. Cancer chemoprevention research with selenium in the post-SELECT era: Promises and challenges. *Nutr. Cancer* **2015**, *68*, 1–17. [[CrossRef](#)]
15. Fritz, H.; Kennedy, D.; Fergusson, D.; Fernandes, R.; Cooley, K.; Seely, A.; Sagar, S.; Wong, R.; Seely, D. Selenium and Lung Cancer: A Systematic Review and Meta Analysis. *PLoS ONE* **2011**, *6*, e26259. [[CrossRef](#)]
16. Kao, R.-H.; Lai, G.-M.; Chow, J.-M.; Liao, C.-H.; Zheng, Y.-M.; Tsai, W.-L.; Hsia, S.; Lai, I.-C.; Lee, H.-L.; Chuang, S.-E.; et al. Opposite Regulation of CHOP and GRP78 and Synergistic Apoptosis Induction by Selenium Yeast and Fish Oil via AMPK Activation in Lung Adenocarcinoma Cells. *Nutrients* **2018**, *10*, 1458. [[CrossRef](#)]
17. Sugita, S.; Ito, K.; Yamashiro, Y.; Moriya, S.; Che, X.-F.; Yokoyama, T.; Hiramoto, M.; Miyazawa, K. EGFR-independent autophagy induction with gefitinib and enhancement of its cytotoxic effect by targeting autophagy with clarithromycin in non-small cell lung cancer cells. *Biochem. Biophys. Res. Commun.* **2015**, *461*, 28–34. [[CrossRef](#)]
18. Wang, Y.-C.; Kulp, S.K.; Wang, D.; Yang, C.-C.; Sargeant, A.M.; Hung, J.-H.; Kashida, Y.; Yamaguchi, M.; Chang, G.-D.; Chen, C.-S. Targeting Endoplasmic Reticulum Stress and Akt with OSU-03012 and Gefitinib or Erlotinib to Overcome Resistance to Epidermal Growth Factor Receptor Inhibitors. *Cancer Res.* **2008**, *68*, 2820–2830. [[CrossRef](#)]
19. Fang, X.; Gu, P.; Zhou, C.; Liang, A.; Ren, S.; Liu, F.; Zeng, Y.; Wu, Y.; Zhao, Y.; Huang, B.; et al.  $\beta$ -Catenin overexpression is associated with gefitinib resistance in non-small cell lung cancer cells. *Pulm. Pharmacol. Ther.* **2014**, *28*, 41–48. [[CrossRef](#)]
20. Kim, Y.M.; Park, S.-Y.; Pyo, H. Cyclooxygenase-2 (COX-2) Negatively Regulates Expression of Epidermal Growth Factor Receptor and Causes Resistance to Gefitinib in COX-2-Overexpressing Cancer Cells. *Mol. Cancer Res.* **2009**, *7*, 1367–1377. [[CrossRef](#)]
21. Liao, C.-H.; Tzeng, Y.-T.; Lai, G.-M.; Chang, C.-L.; Hu, M.-H.; Tsai, W.-L.; Liu, Y.-R.; Hsia, S.; Chuang, S.-E.; Chiou, T.-J.; et al. Omega-3 Fatty Acid-Enriched Fish Oil and Selenium Combination Modulates Endoplasmic Reticulum Stress Response Elements and Reverses Acquired Gefitinib Resistance in HCC827 Lung Adenocarcinoma Cells. *Mar. Drugs* **2020**, *18*, 399. [[CrossRef](#)] [[PubMed](#)]

22. Niu, Q.; Wang, W.; Li, Y.; Ruden, U.M.; Wang, F.; Li, Y.; Wang, F.; Song, J.; Zheng, K. Low Molecular Weight Heparin Ablates Lung Cancer Cisplatin-Resistance by Inducing Proteasome-Mediated ABCG2 Protein Degradation. *PLoS ONE* **2012**, *7*, e41035. [[CrossRef](#)] [[PubMed](#)]
23. Hu, C.F.; Huang, Y.Y.; Wang, Y.J.; Gao, F.G. Upregulation of ABCG2 via the PI3K-Akt pathway contributes to acidic microenvironment-induced cisplatin resistance in A549 and LTEP-a-2 lung cancer cells. *Oncol. Rep.* **2016**, *36*, 455–461. [[CrossRef](#)] [[PubMed](#)]
24. Wang, H.; Zhang, G.; Zhang, H.; Zhang, F.; Zhou, B.; Ning, F.; Wang, H.-S.; Cai, S.-H.; Du, J. Acquisition of epithelial-mesenchymal transition phenotype and cancer stem cell-like properties in cisplatin-resistant lung cancer cells through AKT/ $\beta$ -catenin/Snail signaling pathway. *Eur. J. Pharmacol.* **2014**, *723*, 156–166. [[CrossRef](#)]
25. Kim, K.-C.; Lee, C. Reversal of Cisplatin Resistance by Epigallocatechin Gallate Is Mediated by Downregulation of Axl and Tyro 3 Expression in Human Lung Cancer Cells. *Korean J. Physiol. Pharmacol.* **2014**, *18*, 61–66. [[CrossRef](#)] [[PubMed](#)]
26. Kim, S.; Kim, K.-C.; Lee, C. Mistletoe (*Viscum album*) extract targets Axl to suppress cell proliferation and overcome cisplatin- and erlotinib-resistance in non-small cell lung cancer cells. *Phytomedicine* **2017**, *36*, 183–193. [[CrossRef](#)]
27. Qi, W.; Chen, J.; Cheng, X.; Huang, J.; Xiang, T.; Li, Q.; Long, H.; Zhu, B. Targeting the Wnt-Regulatory Protein CTNNBIP1 by microRNA-214 Enhances the Stemness and Self-Renewal of Cancer Stem-Like Cells in Lung Adenocarcinomas. *Stem Cells* **2015**, *33*, 3423–3436. [[CrossRef](#)]
28. Sun, F.-F.; Hu, Y.-H.; Xiong, L.-P.; Tu, X.-Y.; Zhao, J.-H.; Chen, S.-S.; Song, J.; Ye, X.-Q. Enhanced expression of stem cell markers and drug resistance in sphere-forming non-small cell lung cancer cells. *Int. J. Clin. Exp. Pathol.* **2015**, *8*, 6287–6300.
29. Misuno, K.; Liu, X.; Feng, S.; Hu, S. Quantitative proteomic analysis of sphere-forming stem-like oral cancer cells. *Stem Cell Res. Ther.* **2013**, *4*, 156. [[CrossRef](#)]
30. Park, J.H.; Shin, J.E.; Park, H.W. The Role of Hippo Pathway in Cancer Stem Cell Biology. *Mol. Cells* **2018**, *41*, 83–92. [[CrossRef](#)]
31. Zimmermann, M.; Meyer, N. Annexin V/7-AAD Staining in Keratinocytes. *Methods Mol. Biol.* **2011**, *740*, 57–63. [[CrossRef](#)] [[PubMed](#)]
32. Chou, T.-C. Drug combination studies and their synergy quantification using the Chou-Talalay method. *Cancer Res.* **2010**, *70*, 440–446. [[CrossRef](#)] [[PubMed](#)]
33. Maiuthed, A.; Chantarawong, W.; Chanvorachote, P. Lung Cancer Stem Cells and Cancer Stem Cell-targeting Natural Compounds. *Anticancer Res.* **2018**, *38*, 3797–3809. [[CrossRef](#)] [[PubMed](#)]
34. Eramo, A.; Lotti, F.; Sette, G.; Pilozi, E.; Biffoni, M.; Di Virgilio, A.; Conticello, C.; Ruco, L.; Peschle, C.; De Maria, R. Identification and expansion of the tumorigenic lung cancer stem cell population. *Cell Death Differ.* **2007**, *15*, 504–514. [[CrossRef](#)] [[PubMed](#)]
35. Maji, S.; Panda, S.; Samal, S.K.; Shriwas, O.; Rath, R.; Pellecchia, M.; Emdad, L.; Das, S.K.; Fisher, P.B.; Dash, R. Bcl-2 Antiapoptotic Family Proteins and Chemoresistance in Cancer. *Adv. Cancer Res.* **2018**, *137*, 37–75. [[CrossRef](#)]
36. Liu, X. The Epithelial-Mesenchymal Transition and Cancer Stem Cells: Functional and Mechanistic Links. *Curr. Pharm. Des.* **2015**, *21*, 1279–1291. [[CrossRef](#)]
37. Byers, L.A.; Diao, L.; Wang, J.; Saintigny, P.; Girard, L.; Peyton, M.; Shen, L.; Fan, Y.; Giri, U.; Tumula, P.K.; et al. An Epithelial-Mesenchymal Transition Gene Signature Predicts Resistance to EGFR and PI3K Inhibitors and Identifies Axl as a Therapeutic Target for Overcoming EGFR Inhibitor Resistance. *Clin. Cancer Res.* **2013**, *19*, 279–290. [[CrossRef](#)]
38. Hwang, J.-T.; Kim, Y.M.; Surh, Y.-J.; Baik, H.W.; Lee, S.-K.; Ha, J.; Park, O.J. Selenium Regulates Cyclooxygenase-2 and Extracellular Signal-Regulated Kinase Signaling Pathways by Activating AMP-Activated Protein Kinase in Colon Cancer Cells. *Cancer Res.* **2006**, *66*, 10057–10063. [[CrossRef](#)]
39. Park, S.Y.; Lee, Y.-K.; Kim, H.J.; Park, O.J.; Kim, Y.M. AMPK interacts with  $\beta$ -catenin in the regulation of hepatocellular carcinoma cell proliferation and survival with selenium treatment. *Oncol. Rep.* **2015**, *35*, 1566–1572. [[CrossRef](#)]
40. Shigemitsu, Z.; Manabe, K.; Hara, N.; Baba, Y.; Hosokawa, K.; Kagawa, H.; Watanabe, T.; Fujimuro, M. Methylseleninic acid and sodium selenite induce severe ER stress and subsequent apoptosis through UPR activation in PEL cells. *Chem. Interact.* **2017**, *266*, 28–37. [[CrossRef](#)]
41. Ke, B.; Wei, T.; Huang, Y.; Gong, Y.; Wu, G.; Liu, J.; Chen, X.; Shi, L. Interleukin-7 Resensitizes Non-Small-Cell Lung Cancer to Cisplatin via Inhibition of ABCG2. *Mediat. Inflamm.* **2019**, *2019*, 7241418. [[CrossRef](#)] [[PubMed](#)]
42. D'Amato, T.A.; Landreneau, R.J.; McKenna, R.J.; Santos, R.S.; Parker, R.J. Prevalence of In Vitro Extreme Chemotherapy Resistance in Resected Nonsmall-Cell Lung Cancer. *Ann. Thorac. Surg.* **2006**, *81*, 440–447. [[CrossRef](#)] [[PubMed](#)]
43. Wangpaichitr, M.; Wu, C.; Li, Y.Y.; Nguyen, D.J.M.; Kandemir, H.; Shah, S.; Chen, S.; Feun, L.G.; Prince, J.S.; Kuo, M.T.; et al. Exploiting ROS and metabolic differences to kill cisplatin resistant lung cancer. *Oncotarget* **2017**, *8*, 49275–49292. [[CrossRef](#)] [[PubMed](#)]
44. Duan, W.; Shen, X.; Lei, J.; Xu, Q.; Yu, Y.; Li, R.; Wu, E.; Ma, Q. Hyperglycemia, a Neglected Factor during Cancer Progression. *BioMed Res. Int.* **2014**, *2014*, 461917. [[CrossRef](#)] [[PubMed](#)]
45. Li, W.; Zhang, X.; Sang, H.; Zhou, Y.; Shang, C.; Wang, Y.; Zhu, H. Effects of hyperglycemia on the progression of tumor diseases. *J. Exp. Clin. Cancer Res.* **2019**, *38*, 32. [[CrossRef](#)] [[PubMed](#)]
46. Uprety, B.; Abrahamse, H. Targeting Breast Cancer and Their Stem Cell Population through AMPK Activation: Novel Insights. *Cells* **2022**, *11*, 576. [[CrossRef](#)]
47. Wandee, J.; Prawn, A.; Senggunprai, L.; Kongpetch, S.; Tusskorn, O.; Kukongviriyapan, V. Metformin enhances cisplatin induced inhibition of cholangiocarcinoma cells via AMPK-mTOR pathway. *Life Sci.* **2018**, *207*, 172–183. [[CrossRef](#)]

48. Hirsch, H.A.; Iliopoulos, D.; Tsiachlis, P.N.; Struhl, K. Metformin Selectively Targets Cancer Stem Cells, and Acts Together with Chemotherapy to Block Tumor Growth and Prolong Remission. *Cancer Res.* **2009**, *69*, 7507–7511. [[CrossRef](#)]
49. Brown, J.R.; Chan, D.K.; Shank, J.J.; Griffith, K.A.; Fan, H.; Szulawski, R.; Yang, K.; Reynolds, R.K.; Johnston, C.; McLean, K.; et al. Phase II clinical trial of metformin as a cancer stem cell-targeting agent in ovarian cancer. *JCI Insight* **2020**, *5*, e133247. [[CrossRef](#)]
50. Saini, N.; Yang, X. Metformin as an anti-cancer agent: Actions and mechanisms targeting cancer stem cells. *Acta Biochim. Biophys. Sin.* **2018**, *50*, 133–143. [[CrossRef](#)]
51. Cioce, M.; Pulito, C.; Strano, S.; Blandino, G.; Fazio, V.M. Metformin: Metabolic Rewiring Faces Tumor Heterogeneity. *Cells* **2020**, *9*, 2439. [[CrossRef](#)] [[PubMed](#)]
52. Reid, M.E.; Stratton, M.; Lillico, A.J.; Fakih, M.; Natarajan, R.; Clark, L.C.; Marshall, J.R. A report of high-dose selenium supplementation: Response and toxicities. *J. Trace Elem. Med. Biol.* **2004**, *18*, 69–74. [[CrossRef](#)] [[PubMed](#)]
53. Kuriki, K.; Nagaya, T.; Tokudome, Y.; Imaeda, N.; Fujiwara, N.; Sato, J.; Goto, C.; Ikeda, M.; Maki, S.; Tajima, K.; et al. Plasma Concentrations of (n-3) Highly Unsaturated Fatty Acids Are Good Biomarkers of Relative Dietary Fatty Acid Intakes: A Cross-Sectional Study. *J. Nutr.* **2003**, *133*, 3643–3650. [[CrossRef](#)] [[PubMed](#)]
54. Samuel, S.; Varghese, E.; Kubatka, P.; Triggle, C.; Büsselberg, D. Metformin: The Answer to Cancer in a Flower? Current Knowledge and Future Prospects of Metformin as an Anti-Cancer Agent in Breast Cancer. *Biomolecules* **2019**, *9*, 846. [[CrossRef](#)] [[PubMed](#)]
55. Calza, G.; Nyberg, E.; Mäkinen, M.; Soliymani, R.; Cascone, A.; Lindholm, D.; Barborini, E.; Baumann, M.; Lalowski, M.; Eriksson, O. Lactate-Induced Glucose Output Is Unchanged by Metformin at a Therapeutic Concentration—A Mass Spectrometry Imaging Study of the Perfused Rat Liver. *Front. Pharmacol.* **2018**, *9*, 141. [[CrossRef](#)] [[PubMed](#)]
56. Kajbaf, F.; De Broe, M.E.; Lalau, J.-D. Therapeutic Concentrations of Metformin: A Systematic Review. *Clin. Pharmacokinet.* **2015**, *55*, 439–459. [[CrossRef](#)]
57. Dai, Y.; Liu, S.; Zhang, W.-Q.; Yang, Y.-L.; Hang, P.; Wang, H.; Cheng, L.; Hsu, P.-C.; Wang, Y.-C.; Xu, Z.; et al. YAP1 regulates ABCG2 and cancer cell side population in human lung cancer cells. *Oncotarget* **2016**, *8*, 4096–4109. [[CrossRef](#)]
58. Xia, S.; Duan, W.; Liu, W.; Zhang, X.; Wang, Q. GRP78 in lung cancer. *J. Transl. Med.* **2021**, *19*, 118. [[CrossRef](#)]
59. Wu, Y.; Zhang, H.; Dong, Y.; Park, Y.-M.; Ip, C. Endoplasmic Reticulum Stress Signal Mediators Are Targets of Selenium Action. *Cancer Res.* **2005**, *65*, 9073–9079. [[CrossRef](#)]
60. Gopal, U.; Mowery, Y.; Young, K.; Pizzo, S.V. Targeting cell surface GRP78 enhances pancreatic cancer radiosensitivity through YAP/TAZ protein signaling. *J. Biol. Chem.* **2019**, *294*, 13939–13952. [[CrossRef](#)]
61. Liu, Y.-M.; Wu, T.-H.; Chiu, Y.-H.; Wang, H.; Li, T.-L.; Hsia, S.; Chan, Y.-L.; Wu, C.-J. Positive Effects of Preventive Nutrition Supplement on Anticancer Radiotherapy in Lung Cancer Bearing Mice. *Cancers* **2020**, *12*, 2445. [[CrossRef](#)] [[PubMed](#)]
62. Guo, L.; Cui, J.; Wang, H.; Medina, R.; Zhang, S.; Zhang, X.; Zhuang, Z.; Lin, Y. Metformin enhances anti-cancer effects of cisplatin in meningioma through AMPK-mTOR signaling pathways. *Mol. Ther. Oncolytics* **2020**, *20*, 119–131. [[CrossRef](#)] [[PubMed](#)]
63. Liao, X.-Z.; Gao, Y.; Zhao, H.-W.; Zhou, M.; Chen, D.-L.; Tao, L.-T.; Guo, W.; Sun, L.-L.; Gu, C.-Y.; Chen, H.-R.; et al. Cordycepin Reverses Cisplatin Resistance in Non-small Cell Lung Cancer by Activating AMPK and Inhibiting AKT Signaling Pathway. *Front. Cell Dev. Biol.* **2021**, *8*, 609285. [[CrossRef](#)] [[PubMed](#)]
64. Hampsch, R.A.; Wells, J.D.; Traphagen, N.A.; McCleery, C.F.; Fields, J.L.; Shee, K.; Dillon, L.M.; Pooler, D.B.; Lewis, L.D.; Demidenko, E.; et al. AMPK Activation by Metformin Promotes Survival of Dormant ER+ Breast Cancer Cells. *Clin. Cancer Res.* **2020**, *26*, 3707–3719. [[CrossRef](#)]
65. Andugulapati, S.B.; Sundararaman, A.; Lahiry, M.; Rangarajan, A. AMP-activated protein kinase (AMPK) promotes breast cancer stemness and drug resistance. *Dis. Models Mech.* **2022**, *15*, dmm049203. [[CrossRef](#)]